Extended Abstracts of the 2013 International Conference on Solid State Devices and Materials, Fukuoka, 2013, pp334-335

The Numerical Model Fitting and Transient Luminescence Analysis for Understanding Degradation Mechanism in Phosphorescent Blue Organic Light Emitting Diodes (OLEDs)

Tadahiko Hirai, Karl Weber, Jenny O'Connell, Mark Bown and Kazunori Ueno

Materials Science and Engineering, CSIRO
Bayview Avenue, Clayton, Victoria 3168, Australia
Phone: +61-3-9545-7814 E-mail: tadahiko.hirai@csiro.au

1. Introduction

Recently, significant progress has been made in the performance of OLED, particularly with regard to their brightness and lifetime. OLEDs are now a viable technology for the manufacture of large-area flat panel displays (FPD) to compete with Liquid Crystal Display (LCD) and plasma technologies. However, the operating mechanisms including charge-injection, -transport, -trapping, and -recombination phenomena in organic semiconductors are still unclear and require further investigation.

A common approach to estimate the barrier height of an organic-conductor interface is to apply the Richardson-Schottky model [1-2] with the value of the Richardson Factor (*A**) set for a silicon-metal interface. On the other hand, other groups have reported methods for the demonstration of device parameters such as carrier mobility, Density of State (DOS) and barrier height.[3]

We have previously described a novel numerical model for fitting the methodologies of Schottky[10] and impedance spectroscopy (IS) to be a useful tool for evaluating relaxation, transport and injection phenomena in a variety of organic devices.[4-7] And, we have also proposed a new blue phosphorescent iridium complex.[8]

In this paper, we report analysis of degradation phenomena after current stress in comparison between phosphorescent materials. Our key methodologies for analysis are numerical model fitting of novel Schottky model and transient measurement of pulsed luminescence.

2. Theory

2.1. Modified Schottky Model

The current density of a Schottky organic-conductor interface may be expressed as**:**

$$J_{inj} = A^* T^2 \exp\left(\frac{-e\left(\phi_B - \sqrt{eE/4\pi\varepsilon_i}\right)}{k_B T}\right) \quad (1)$$

$$A^* = \frac{16\pi\varepsilon\varepsilon_0 N_0 \mu k_B^{\,2}}{e^2} \quad [A/cm^2K^2] \quad (2)$$

where, *A**, *T*, *e*, ϕ_B, *E*, ε_0, ε, k_B, N_0, and μ are the Richardson factor, temperature, electron charge, barrier height, applied electric field, permittivity of vacuum, relative permittivity, Boltzmann constant, state density and carrier mobility, respectively. The value for *A** as proposed by Scott is dependent on N_0 and μ of the organic material. We have modified the Schottky equation to include ϕ_B and a non-zero electric field.

2.2. Complex Capacitance Model for IS

The real and imaginary part of capacitance are described as follows ;

$$C_R(\omega) = \frac{1}{2R_j\delta\omega}\frac{B}{(1+A)^2+B^2} \quad (3)$$

$$C_I(\omega) = \frac{S D_{it}}{2\omega d\delta} v_{th} S_t C_0 V \exp\left(\frac{-q\left(\phi_B - \sqrt{qE/4\pi\varepsilon_i}\right)}{k_B T}\right) \ln\left(1+\omega^2\tau^2\right) \quad (4)$$

where, C_R, C_I, ω, *S*, *d*, R_i, δ, v_{th}, S_t, C_0, *V*, *q*, D_{it}, and τ are the real part of capacitance, imaginary part of capacitance, angular frequency, active area, thickness of organic semiconductor, the low-frequency incremental resistance of the diode, the trapping parameter, the thermal carrier velocity, the capture cross-section, the static electric capacitance of the organic layer, the bias voltage, the electron charge, the interface state density and the time constant for the characteristic time required to fill & empty the interface state, respectively.

The variables *A* and *B* are expressed as follows:

$$A = N_t(E_0) S_t v_{th} \frac{k_B T\pi}{2\omega}$$

$$\frac{d\omega B}{d\omega} = N_t(E_0) S_t v_{th} \frac{k_B T\pi}{\omega}$$

$$N_t(E_0) = N_0 \exp\left(-\frac{T_0}{T}\ln\frac{N_V S_t v_{th}}{\omega}\right)$$

where, $N_t(E_0)$ is the energy distribution of the localized state density at the valence band edge, N_V is the effective density of state in the valence band and N_0 is the density of localized states at the valence band edge (DOS).

3. Experimental

3.1. HOD and EOD

We fabricated a hole-only device (HOD) ; glass / ITO (150nm) / TcTa (70nm) / Al (150nm) and an electron-only device (EOD) ; glass / ITO (150nm) / TmPyPB (70nm) /LiF (1nm) / Al (150nm).

Temperature dependent I-V characteristics were obtained, under vacuum (1×10^{-2} Pa), with a temperature controlled probe system in order to estimate ϕ_B and *A**. Carrier mobility was calculated using the dark injection (DI) – space charge limited current (SCLC) method [9]. A Solartron SI-1255 and 1296 frequency response analyzer system were used for IS measurements.

3.2. Phosphorescence blue OLED

We fabricated a phosphorescent blue OLED having combination of mCP or MMH-001[8] as host materials, and FIrpic or MMPBD-001[8] as guest materials. Table I. shows variation of the device structures in this report in-

cluding partially doped structure in emission layer.

Device	Structure (Thickness[nm], Concentration wt%)
A	ITO/TcTa(70)/mCP:FIrpic(40, 6%)/TmPyPB(40)/LiF(1)/Al
B	ITO/TcTa(70)/MH1:FIrpic(40, 6%)/TmPyPB(40)/LiF(1)/Al
C	ITO/TcTa(70)/MH1:MPBD1(40, 6%)/TmPyPB(40)/LiF(1)/Al
D	ITO/TcTa(70)/MH1(20)/MH1:MPBD1(20, 6%)/TmPyPB(40)/LiF(1)/Al
E	ITO/TcTa(70)/MH1(2)/MH1:MPBD1(20, 6%)/MH1(18)/TmPyPB(40)/LiF(1)/Al

Table I. The variation of OLEDs structures (A-C; Host/Guest variation, D-E; Partial doping). MH1=MMH-001[8], MPBD1=MMPBD-001[8]

Luminescence and I-V characteristics were obtained with a luminescence colour meter (Topcon BM-7A) and a source-measure unit (Keithley 2400).

3.3 Transient luminescence measurement

Transient luminescence responses were obtained with a photomultiplier (Hamamatsu H10421) and a digital storage oscilloscope (Rigol DS1202CA), in pulsed operation by a function wave form generator (Rigol DG1022).

3.4 Stress tests

We compare device performances with the parameters and transient responses between before and after current stress (1hr at 5mA/cm^2).

4. Results and Discussion

4.1 Determination of Device Parameters

Using fits to the numerical model, we have estimated ϕ_B(H)=0.33 [eV] and A^*(H)=1.0×10^{-3} [A/cm^2/K^2] for the injection of hole carriers. We have estimated D_{it}(H)=5.0×10^8[/cm^2] and H_0(H)=1.0×10^{16}[/cm^{3}eV] for the hole injection side.

We also obtained the device parameters for the electron injection interface from the temperature dependent I-V characteristics of the EOD ; ϕ_B(E)=0.65 [eV], A*(E)= 1.0×10^2 [A/cm^2/K^2], D_{it} (E)=5.0×10^{11} [/cm^2] and H_0 (E)=2.0×10^{18} [/cm^{3}eV].

4.2. Characterization of phosphorescent blue OLED

We obtained highly efficient blue luminescence from our OLEDs. The typical parameters are shown in Table II. Device C having a combination of MMH-001:MMPBD-001 as emission layer emits a deeper blue colour than the FIrpic based devices.

Device	V_{ON}[V]	L*[cd/m^2]	L/J*[cd/A]	η*[lm/W]	CIE_{1931}* (x, y)
A	3.4	248	24.8	13.4	(0.16, 0.31)
B	3.2	238	23.8	13.6	(0.17, 0.32)
C	3.0	264	26.4	14.4	(0.15, 0.21)

Table II. The V-I-L performance depending on variation of OLEDs structures. *) Data in case of current bias 1 mA/cm^2

Where, V_{ON}, L, L/J, η, and CIE_{1931} are the turn-ON voltage (at 1cd/m^2), the luminescence, the current efficiency, the power efficiency and the CIE coloure index, respectively.

4.3. Device parameters before/after current stress

Device	before current stress		after current stress	
	V_{ON}[V]	D_{IT} [/cm^2]	V_{ON}[V]	D_{IT} [/cm^2]
A	3.2	4×10^6	4.2	5×10^7
B	3.2	4×10^3	3.6	5×10^4
C	3.2	5×10^5	4.6	5×10^5

Table III. The changing of the turn-on voltage (V_{ON}) and the estimated interface trap density (D_{IT}).

Several device parameters changed after current stress. Comparison of the turn-ON voltage (V_{ON}) and the interface trap density (D_{IT}) before and after current stress is shown in Table III. Only Device-C exhibits no change of D_{IT} before and after current stress.

4.4. Transient luminescence before/after current stress

The transient analysis of pulsed luminescence for deep blue Devices C, D and E before and after current stress is shown in Figure 1. A delay of rise time and positive shift of turn-ON voltage (V_{ON}) are observed after current stress in all devices.

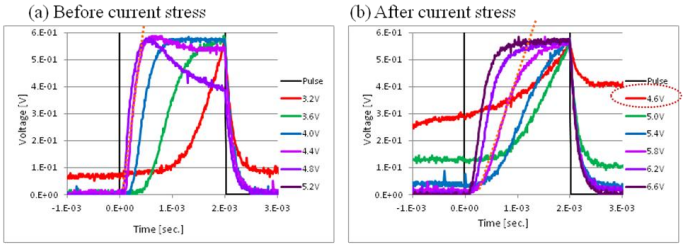

Figure 1. The result of transient luminescence measurement of Device-C before and after current stress.

In the case of partially doped devices D and E, Device-E having close contact between the doped emissive layer and the hole injection interface shows a delayed rise time. We believe the mechanism of trap and release was generated at the hole injection interface after current stress.

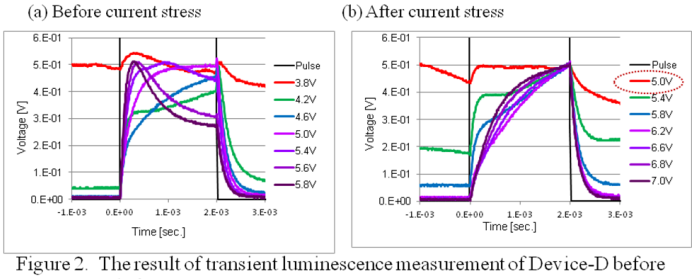

Figure 2. The result of transient luminescence measurement of Device-D before and after current stress.

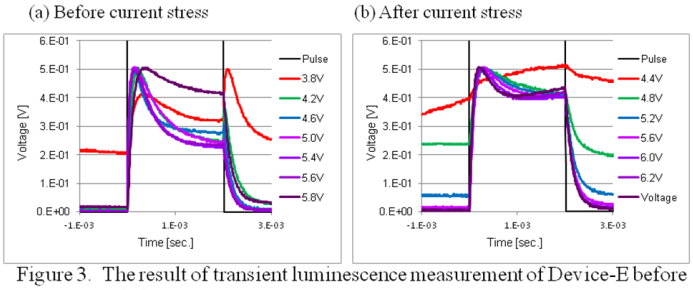

Figure 3. The result of transient luminescence measurement of Device-E before and after current stress.

References

[1] O. W. Richardson, *Philos. Mag.* **28,** 633 (1914).

[2] J.C. Scott *J.Vac.Sci.Tech.* **A21,** 521A (2003).

[3] T. Okachi, T. Nagase, T. Kobayashi, and H. Naito: *Jpn. J. Apple. Phys.* **47**, 8965 (2008).

[4] T. Hirai, K. Weber, J. H. Li, M. Bown and K. Ueno, *2011 SID International Symposium* P181.

[5] T. Hirai, K. Weber, J. O'Connell, M. Bown and K. Ueno, *2011 SSDM International Symposium* B-1-6.

[6] T. Hirai, K. Weber, J. O'Connell, M. Bown and K. Ueno, *2012 SSDM International Symposium* M-3-3.

[7] T. Hirai, K. Weber, J. O'Connell, M. Bown and K. Ueno, *Jpn. J. Apple. Phys.* **52**, 04CK02 (2013).

[8] M. Groarke, S. Andresen, J. O'Connell, T. Hirai, K. Weber, J. H. Li, J. MacDonald, M. Bown and K. Ueno, *J.SID.* **20**, 70 (2012)

[9] S. C. Tse, S. W. Tsang, and S. K. So, *J. Appl. Phys.* **100**, 063708 (2006).

[10] S. M. Sze *Physics of Semiconductor Devices 2nd Edition* , 257